# Single Low-Dose Injection of Evans Blue Modified PSMA-617 Radioligand Therapy Eliminates Prostate-Specific Membrane Antigen Positive Tumors

Zhantong Wang,[†] Rui Tian,[†] Gang Niu,[†] Ying Ma,[†] Lixin Lang,[†] Lawrence P. Szajek,[‡] Dale O. Kiesewetter,[†] Orit Jacobson,*[,†] and Xiaoyuan Chen*[,†]

[†]Laboratory of Molecular Imaging and Nanomedicine, National Institute of Biomedical Imaging and Bioengineering, National Institutes of Health, Bethesda, Maryland, United States

[‡]Positron Emission Tomography Department, Warren Grant Magnuson Clinical Center, National Institutes of Health, Bethesda, Maryland, United States

S Supporting Information
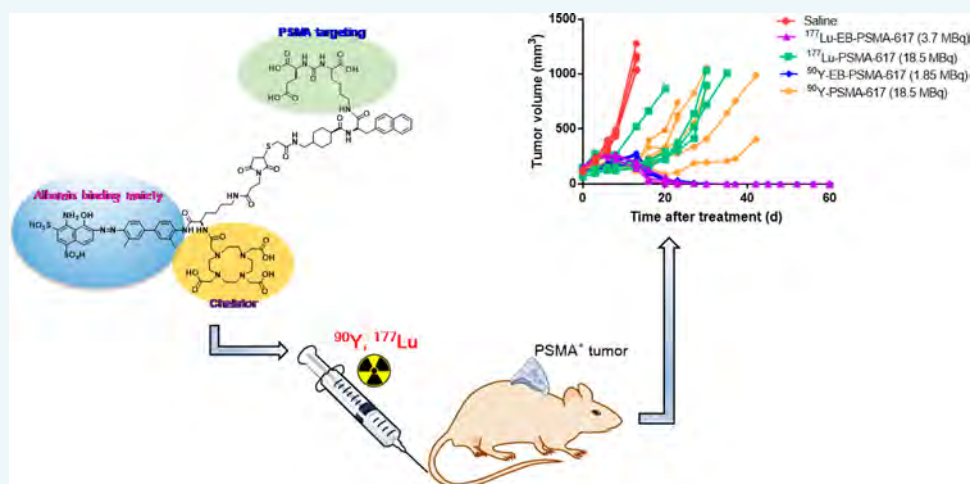
ABSTRACT: Prostate cancer is the most frequently diagnosed malignant tumor in men worldwide. Prostate-specific membrane antigen (PSMA) is a surface molecule specifically expressed by prostate tumors that has been shown to be a valid target for internal radionuclide therapy in both preclinical and clinical settings. The most common radiotherapeutic agent is the small molecule ^{177}Lu-PSMA-617, which is under clinical evaluation in multiple countries. Nevertheless, its efficacy in causing tumor regression is still suboptimal, even when administered in several cycles per patient, perhaps due to poor pharmacokinetics (PK), which limits uptake by the tumor cells. We postulated that the addition of the Evans blue (EB) moiety to PSMA-617 would improve the PK by extending circulation half-life, which would increase tumor uptake and improve radiotherapeutic efficacy. PSMA-617 was modified by conjugation of a 2-thiol acetate group onto the primary amine and thereafter reacted with a maleimide functional group of an EB derivative, to give EB-PSMA-617. The PK and radiotherapeutic efficacy of [90]Y- or ^{177}Lu-EB-PSMA-617 was compared to the clinically used radiopharmaceutical [90]Y- or [177]Lu- PSMA-617 in PC3-PIP tumor-bearing mice. EB-PSMA-617 retained binding to serum albumin as well as a high internalization rate by tumor cells. Upon injection, metal-labeled EB-PSMA-617 demonstrated an extended blood half-life compared to PSMA-617 and, thereby, prolonged the time window for binding to PSMA. The improved PK of EB-PSMA-617 resulted in significantly higher accumulation in PSMA[+] tumors and highly effective radiotherapeutic efficacy. Remarkably, a single dose of 1.85 MBq of [90]Y- or ^{177}Lu-EB-PSMA-617 was sufficient to eradicate established PMSA[+] tumors in mice. No significant body weight loss was observed, suggesting little to no gross toxicity. The construct described here, EB-PSMA-617, may improve the radiotherapeutic efficacy for patients with PSMA-positive tumors by reducing both the amount of activity needed for therapy as well as the frequency of administration, as compared to PSMA-617.

INTRODUCTION

Prostate cancer is the most frequently diagnosed malignant tumor in men worldwide. Prostate-specific membrane antigen (PSMA) is a surface molecule predominately expressed by
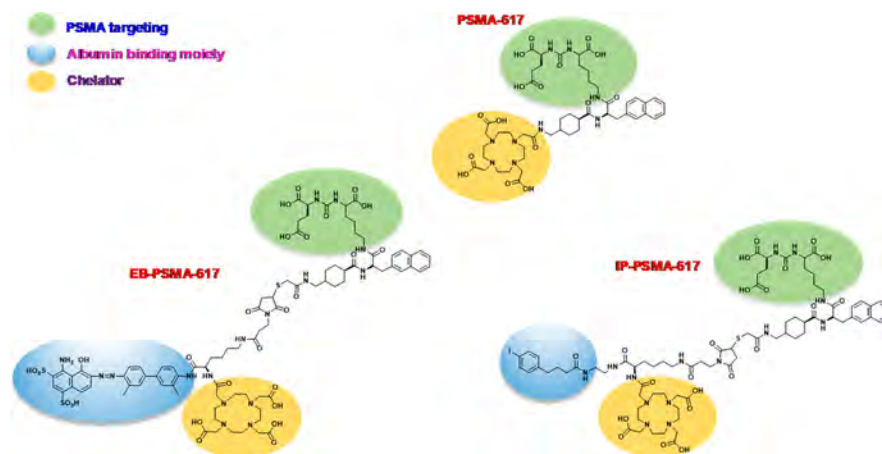
Figure 1. Chemical structures of PSMA-617, EB-PSMA-617, and IP-PSMA-617. Serum albumin motifs are marked in blue circle. PSMA-specific ligand is shown in a green circle. Chelator for labeling is marked in yellow circle.

prostate tumor cells, and its expression level correlates with disease stage and with conversion to hormone-refractory cancers.[1−7] PSMA is expressed at lower concentrations in the normal prostate, and minor amounts are also observed in the brain, kidneys, salivary glands, and small intestine. The antigen was also shown to be expressed by neovascular tumor vessels of multiple other cancers.[1−4,8]

High expression of PSMA in advanced stages of prostate cancer and metastatic castration-resistant prostate cancer (mCRPC) makes it an important target for imaging and therapeutic treatment. The membrane expression of PSMA has led to multiple strategies targeting the antigen in order to deliver therapy for the disease, including vaccines, specific antibodies, antibody−drug conjugates, and radionuclide therapy.[1,7,9−12]

In human patients, the anti-PSMA antibody labeled with ^{177}Lu (physical $t_{1/2}$ = 6.65 days, β = 0.497 MeV, γ = 0.208 MeV, particle penetration range in the live tissue of 1.5 mm) or ^{90}Y (physical $t_{1/2}$ = 2.67 days, β = 2.28 MeV, particle penetration range in the live tissue of 12 mm) was shown to be an effective agent, but had bone marrow and hematological toxicity, possibly due to its long retention in the blood (days).[1,13−17]

PSMA was found to be highly homologous to N-acetyl-L-aspartyl-L-glutamate peptidase I, a neuropeptidase that produces the neurotransmitter glutamate and N-acetylaspartate (NAA) through the hydrolysis of N-acetylaspartylglutamate (NAAG).[18,19] This finding led to the design and development of various classes of small molecule ligands to PSMA based on different structural motifs, such as phosphorus esters, carbamates, and ureas.[3] The most widely used for imaging and therapy are the urea ligands that are constructed of three components: the binding motif (of which glutamate-urea-lysine [Glu-urea-Lys] is the most widely used scaffold), a linker, and a radiolabel-bearing moiety (chelator molecule for radiolabeling).[3] Upon binding to PSMA, the ligands are internalized. Receptor recycling increases the deposition of radioisotopes, leading to enhanced tumor uptake, retention, and subsequent high image quality for diagnosis and high local doses for therapy.[3,20,21] However, similarly to other small-molecule-based imaging tracers, these PSMA ligands display rapid clearance from the circulation, which confers a low background early after injection but significantly limits accumulation in prostate cancer tumors.[3,10]

Several small molecules targeting PSMA, labeled with radiotherapeutic beta emitters such as Lu-177, were evaluated in prostate cancer patients.[1] The most commonly used small molecule, ^{177}Lu-PSMA-617, is currently under clinical evaluation in multiple countries. In the ^{177}Lu-PSMA-617 clinical trials, patients are typically treated with 3−8 GBq per single injection and up to six cycles.[1,22−24] The limited available data suggest partial response rates of up to 70−80% that were limited to as few as several weeks in some of the patients.[25,26] Encouragingly, only stage 1−2 hematologic toxicities and sporadically mild xerostomia and fatigue were reported as adverse effects, but the long-term toxicity is yet unknown.[1,22,23,25,26]

Several attempts to enhance the blood half-life of small molecules (such as PSMA-617 and other low molecular weight PSMA ligands) and peptides by reversible binding to albumin have been reported.[27−35] The overall concept is to conjugate the target molecule to a moderate affinity albumin binding moiety such as Evans blue (EB) or 4-(p-iodophenyl)butyric acid (IP).[27−35]

The aim of this study was to improve the tumor uptake and treatment efficacy of PSMA-617 through an increase of its blood circulation half-life, by covalently attaching PSMA-617 to an albumin-binding Evans blue (EB) derivative.[34,35] Importantly, attachment of EB extends the blood half-life to several hours, which is significantly shorter than the half-life of the PSMA antibody mentioned above and therefore should not have similar toxicities observed with PSMA-specific antibody radiotherapy.

In vitro properties as well as pharmacokinetic characteristics of the three radiopharmaceuticals were evaluated, and the superiority of EB-PSMA-617 and IP-PSMA-617 over PSMA-617 was demonstrated. Interestingly, EB-PSMA-617 was internalized and retained in tumor cells significantly better than IP-PSMA-617. Treatment efficacy of EB-PSMA-617 in the PSMA$^+$ xenograft model at escalating doses showed that a low single dose injection, 1.85 MBq ^{90}Y-EB-PSMA-617 or 3.7 MBq ^{177}Lu-EB-PSMA-617, was sufficient to eradicate existing tumors.

■ RESULTS

Chemistry and Radiolabeling. Synthesis of the PSMA-617 conjugate to the DOTA chelator was done similarly to the published literature, using DOTA-NHS ester.[36] Exploring

bifunctional tracer designs was reported by others.[37,38] In our design, to introduce the albumin binding motif onto PSMA-617, it was modified to have a free thiol group on the primary amine. The thiol was covalently attached to the maleimide-albumin binding motifs, to give EB-PSMA-617 or IP-PSMA-617 derivatives (Figure 1). More details on the synthetic scheme and analysis are available in the Supporting Information (Figures S1−S6). The radioligands were labeled in one step, with radiochemical purities >98% for all three radioisotopes: ^{86}Y, ^{90}Y, and ^{177}Lu, as determined by radioTLC, with specific activities of 150−220 MBq/μmol.

Cell-Based PSMA Receptor Binding Assay. Expression of PSMA in both PC3 (PSMA$^-$) and PC3-PIP (PSMA$^+$) cell lines was verified by flow cytometry (Figure 2A). All three
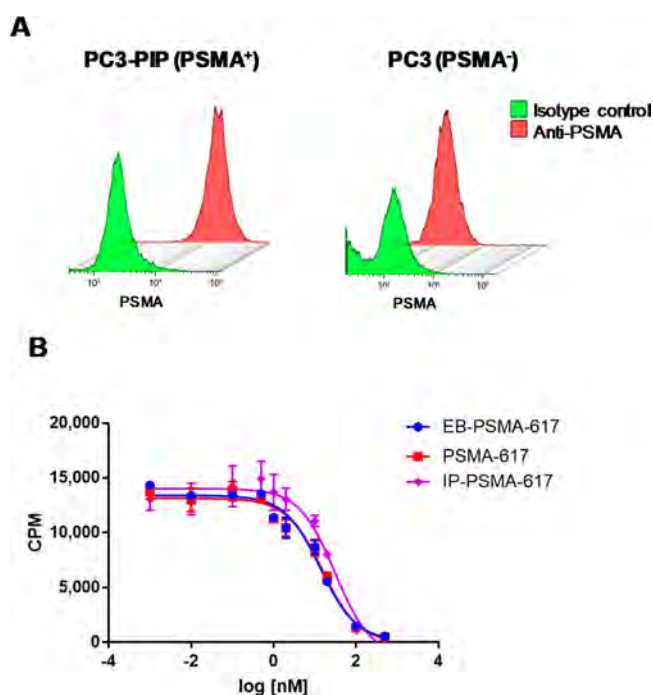

Figure 2. (A) Representative histograms of PSMA expression evaluated by flow cytometry in PC3-PIP (PSMA$^+$) and PC3 (PSMA$^-$) cells. (B) Cell binding affinity assays of PSMA-617, EB-PSMA-617, and IP-PSMA-617 in PSMA$^+$ cells. IC$_{50}$ of PSMA-617 (red curve): 15.4 nM. IC$_{50}$ of EB-PSMA-617 (blue curve): 13.7 nM. IC$_{50}$ of IP-PSMA-617 (purple curve): 30.1 nM. Results are shown as average ± SD of triplicates.

ligands exhibited similar cell binding affinities to PSMA, with IC$_{50}$ values of 13.7, 15.4, and 30.1 nM for EB-PSMA-617, PSMA-617, and IP-PSMA-617, respectively (Figure 2B).

Uptake, Internalization, and Efflux Assays. All three radioligands had rapid uptake after 1 h incubation in PSMA$^+$ cells, while ^{86}Y-IP-PSMA-617 had slightly higher uptake (7.6 ± 0.3%AD) than ^{86}Y-EB-PSMA-617 (5.6 ± 0.1%AD) and ^{86}Y-PSMA-617 (4.2 ± 0.2%AD; Figure 3A). The uptake for all radioligands increased over time, reaching a maximum value at 24 h after incubation with values of 17.2 ± 1.8, 27.1 ± 0.8, and 9.3 ± 0.4% AD for ^{86}Y-IP-PSMA-617, ^{86}Y-EB-PSMA-617, and ^{86}Y-PSMA-617, respectively (Figure 3A). Using an excess amount of unlabeled ligand significantly reduced the uptake to the level observed in PSMA$^+$ PC3 cells (Figure 3A, $P < 0.01$), indicating the specificity of the radioligands to PSMA. The uptake of the radioligands in PSMA$^-$ cells was significantly

lower ($P < 0.01$) than that of PSMA$^+$ cells (Figure S7). Out of the three radioligands, ^{86}Y-EB-PSMA-617 was most effectively internalized, reaching an average of 80% at a 24 h time point (Figure 3B). ^{86}Y-PSMA-617 exhibited the lowest internalization degree (about 44% at 24 h time point, Figure 3B). The internalization proportion of two albumin binding radioligands, ^{86}Y-EB-PSMA-617 and ^{86}Y-IP-PSMA-617, increased over time (Figure 3B). Interestingly, a higher efflux rate was found for ^{86}Y-PSMA-617 and ^{86}Y-IP-PSMA-617 over ^{86}Y-EB-PSMA-617 (Figure 3C).

PET Studies. To investigate the pharmacokinetics of PSMA-617, EB-PSMA-617, and IP-PSMA-617, we performed PET studies over time using the PET radioisotope Y-86 ($t_{1/2}$ 14.7 h, 33% positron emitter, Figure 4). The albumin binding radioligands, ^{86}Y-EB-PSMA-617 and ^{86}Y-IP-PSMA-617, showed higher tumor uptake than ^{86}Y-PSMA-617 at 4, 24, and 48 h p.i. (Figures 4 and 5A). Compared to ^{86}Y-PSMA-617, which rapidly cleared from the blood, ^{86}Y-EB-PSMA-617 and ^{86}Y-IP-PSMA-617 exhibited significantly ($P < 0.01$) longer blood circulation (12.2 ± 0.8% ID/g and 11.9 ± 1.4% ID/g at 1 h p.i. for ^{86}Y-EB-PSMA-617 and ^{86}Y-IP-PSMA-617; Figures 4 and 5B). Comparison between the two albumin-binding radioligands implied that ^{86}Y-EB-PSMA-617 had slower blood clearance ($t_{1/2}$ 5.6 h) than ^{86}Y-IP-PSMA-617 ($t_{1/2}$ 2.1 h). The tumor uptake of ^{86}Y-IP-PSMA-617 was higher than that of ^{86}Y-EB-PSMA-617 at the 4 h time point (65.6 ± 9.1% ID/g vs. 40.9 ± 6.7% ID/g, Figure 5A). It is striking that tumor uptake of ^{86}Y-EB-PSMA-617 was retained over time (74.5 ± 11.0% ID/g at 24 h and 77.3 ± 6.2% ID/g at 48 h), whereas the tumor uptakes of ^{86}Y-IP-PSMA-617 and ^{86}Y-PSMA-617 significantly decreased ($P < 0.01$) over time (Figure 5A). Note that kidney uptake of ^{86}Y-EB-PSMA-617 also increased over time, reaching a plateau at 24 h p.i., which remained steady over time, while most of ^{86}Y-IP-PSMA-617 and ^{86}Y-PSMA-617 was cleared from the kidneys within 4 and 1 h, respectively (Figures 4 and 5C). Kidney uptake of ^{86}Y-EB-PSMA-617 was about 3-fold lower than the PC3-PIP tumor (Figures 4A and 5A and C). This kidney uptake was blocked (64% blocking) by coinjection of ^{86}Y-EB-PSMA-617 and an excess amount of unlabeled EB-PSMA-617 (Figure S8A), indicating PSMA specificity of ^{86}Y-EB-PSMA-617 accumulation in the renal cortex.[39] Moreover, injection of ^{86}Y-EB-PSMA-617 to PSMA$^-$ tumor mice resulted in significantly lower tumor uptake but similar kidney uptake to that in PSMA$^+$ tumor mice (Figure S8B). These PET results were further verified by direct tissue sampling biodistribution studies (Figures S9 and S10).

Radiotherapy Studies of ^{90}Y/^{177}Lu-Labeled EB-PSMA-617 and PSMA-617. The high tumor uptake and internalization rate of EB-PSMA-617 over IP-PSMA-617 and PSMA-617 encouraged us to evaluate its therapeutic efficacy by a single low dose administration (Figure 6A and B). A single dose injection as low as 1.85 MBq of ^{90}Y-EB-PSMA-617 or 3.7 MBq of ^{177}Lu-EB-PSMA-617 eradicated the tumor completely within 27 days post-treatment (Figure 6A and B). One-hundred percent survival and no significant ($P > 0.01$) drop in body weight suggest negligible systemic toxicity of the radioligands (Figures S11 and S12).

Mice bearing PSMA$^+$ xenografts, which were treated with similar doses of ^{90}Y-IP-PSMA-617 and ^{177}Lu-IP-PSMA-617, did not eradicate existing tumors as per their EB-PSMA-617 counterparts (Figure 6A and B). Out of six mice injected with 1.85 MBq of ^{90}Y-IP-PSMA-617, only one mouse had a
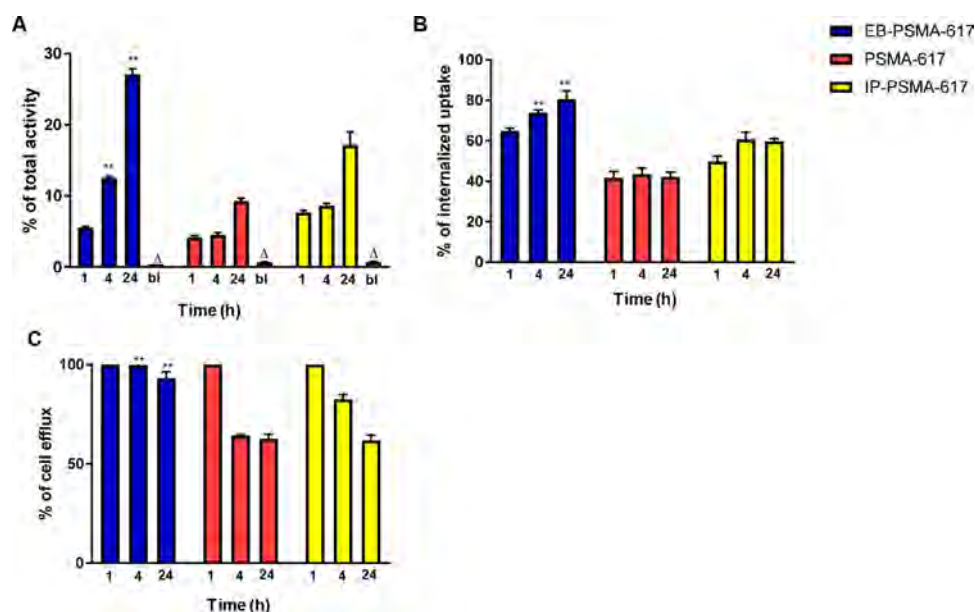
Figure 3. Uptake, internalization, and efflux of ^{86}Y-EB-PSMA-617, ^{86}Y-PSMA-617, and ^{86}Y-IP-PSMA-617 in PSMA$^+$ PC-3-PIP cells in the presence of 1% (w/v) human serum albumin. (A) % of total activity consumed by cells over time. bl, blocking studies at 24 h. (B) % of internalized uptake and (C) % of efflux over time. Results are shown as average ± SD of triplicates. ΔP < 0.01 radiotracer uptake vs blocking at 24 h, **P < 0.01 ^{86}Y-EB-PSMA-617 vs ^{86}Y-IP-PSMA-617 and ^{86}Y-PSMA-617 at 4 and 24 h time points.
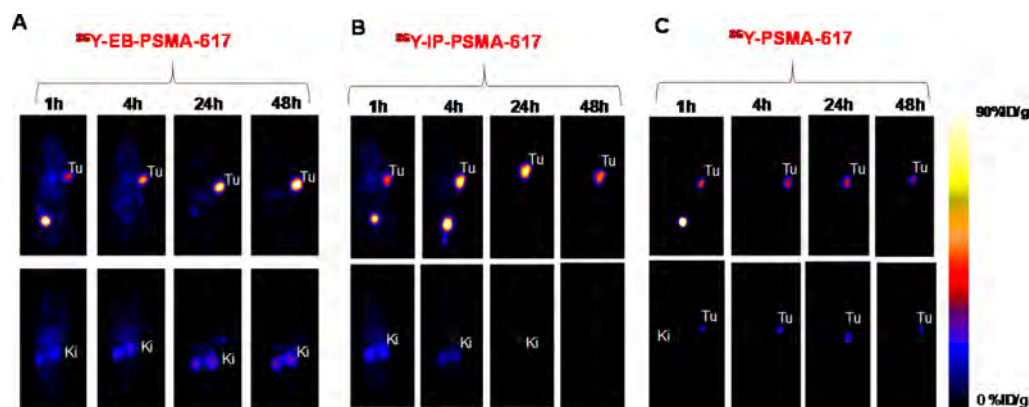

Figure 4. Representative coronal PET images of PSMA$^+$ tumor model, injected with 3−3.7 MBq of ^{86}Y-EB-PSMA-617 (A), ^{86}Y-IP-PSMA-617 (B), or ^{86}Y-PSMA-617 (C) over time. Upper panel is ventral slices. Lower panel is dorsal slices. All the images were normalized to % ID/g ranging from 0 to 90. Tu, tumor; K_i, kidneys.

complete tumor remission (16.6% survival), and mice injected with 3.7 MBq ^{177}Lu-IP-PSMA-617 had tumor growth inhibition compared to the saline group, but the tumors regrew, and the mice did not survive.

Moreover, higher doses of PSMA-617 (7.4 MBq of ^{90}Y-PSMA-617 or 37 MBq of ^{177}Lu-PSMA-617) resulted in partial tumor regression as compared to the control group injected with saline (Figure 6C and D). In the ^{177}Lu-PSMA-617 group injected with a high dose of 37 MBq, one mouse (20%) had complete tumor regression. The other four tumors in this group continued to grow since day 30 post-treatment and were not significantly different from the control group or the other ^{177}Lu/^{90}Y-PSMA-617 groups by the end of this study (Figure 6C and D and Figures S11 and S12).

The PSMA specificity of ^{90}Y-EB-PSMA-617 and ^{177}Lu-EB-PSMA-617 treatment was evaluated by injecting high doses (7.4 MBq of ^{90}Y-EB-PSMA-617 and 18.5 MBq of ^{177}Lu-EB-PSMA-617) to PSMA$^-$ PC3 tumor mice, which did not result

in tumor eradication, as was seen in PSMA$^+$ PC3-PIP tumor mice (Figure 6A and B).

Immunofluorescence staining found a reduced level of PSMA expression, reduction in proliferation rate (K_i-67), and higher DNA damage/cell apoptosis (TUNEL) for the PC3-PIP tumor mice treated with ^{90}Y-EB-PSMA-617 or ^{177}Lu-EB-PSMA-617 over the control, ^{90}Y-PSMA-617, and ^{177}Lu-PSMA-617 groups (Figures S13−S16). These results were not achieved in PSMA$^-$ PC3 tumor mice (Figure S17). Blood analysis for EB-PSMA-617 treated groups showed no significant difference over the control groups (Table 1). Moreover, pathologic examination of H&E staining of the tumor and selected noncancerous organs displayed no obvious abnormalities (Figures S18 and S19).

■ **DISCUSSION**

PSMA-617 radionuclide therapy is a successful treatment with regard to prostate specific antigen (PSA) reduction; however, it requires multiple doses administered to the patient, and its
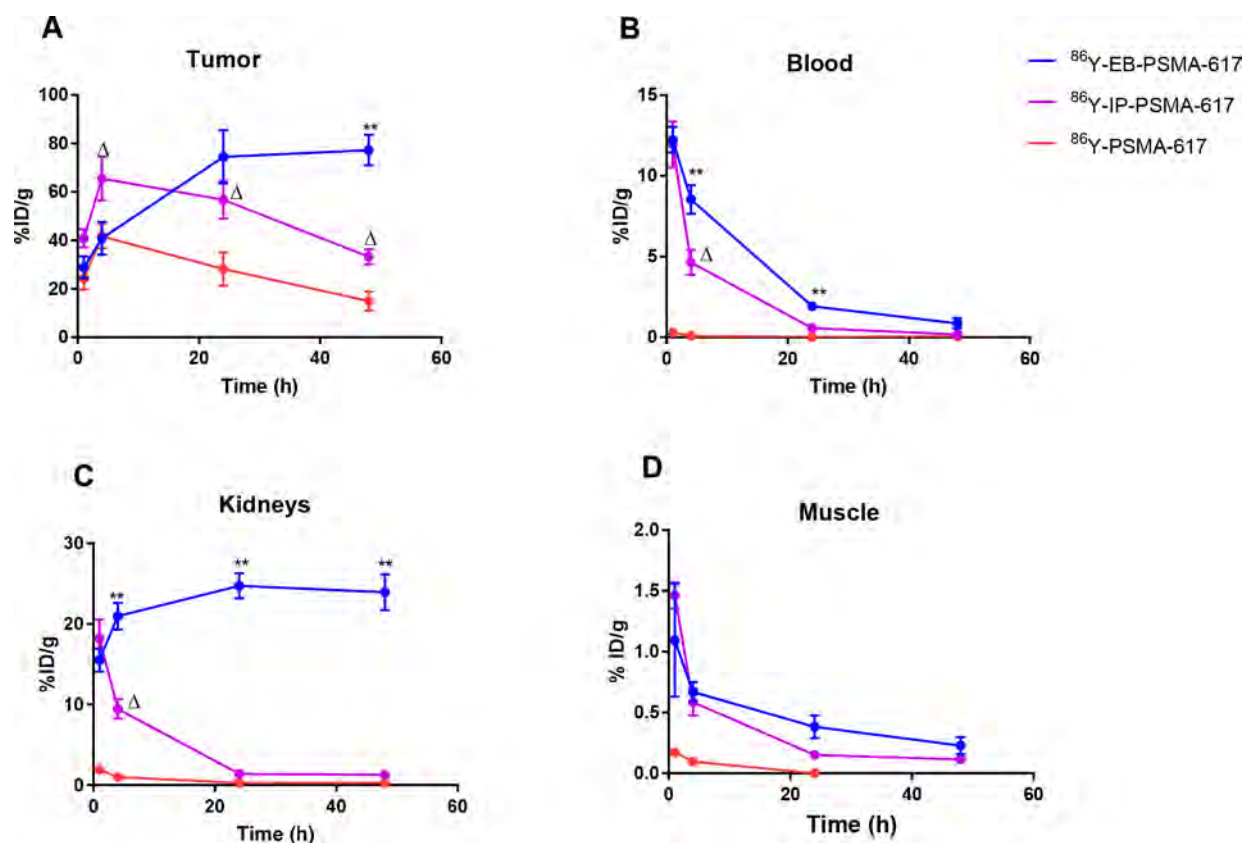
Figure 5. Time activity curves (decay corrected) of [86]Y-EB-PSMA-617, [86]Y-IP-PSMA-617 and [86]Y-PSMA-617 in tumor (A), blood (B) kidneys (C) and muscle (D) in PSMA[+] tumor model. **$P < 0.01$ [86]Y-EB-PSMA-617 vs. [86]Y-IP-PSMA-617 and [86]Y-PSMA-617. Δ$P < 0.01$ [86]Y-IP-PSMA-617 vs. [86]Y-PSMA-617.
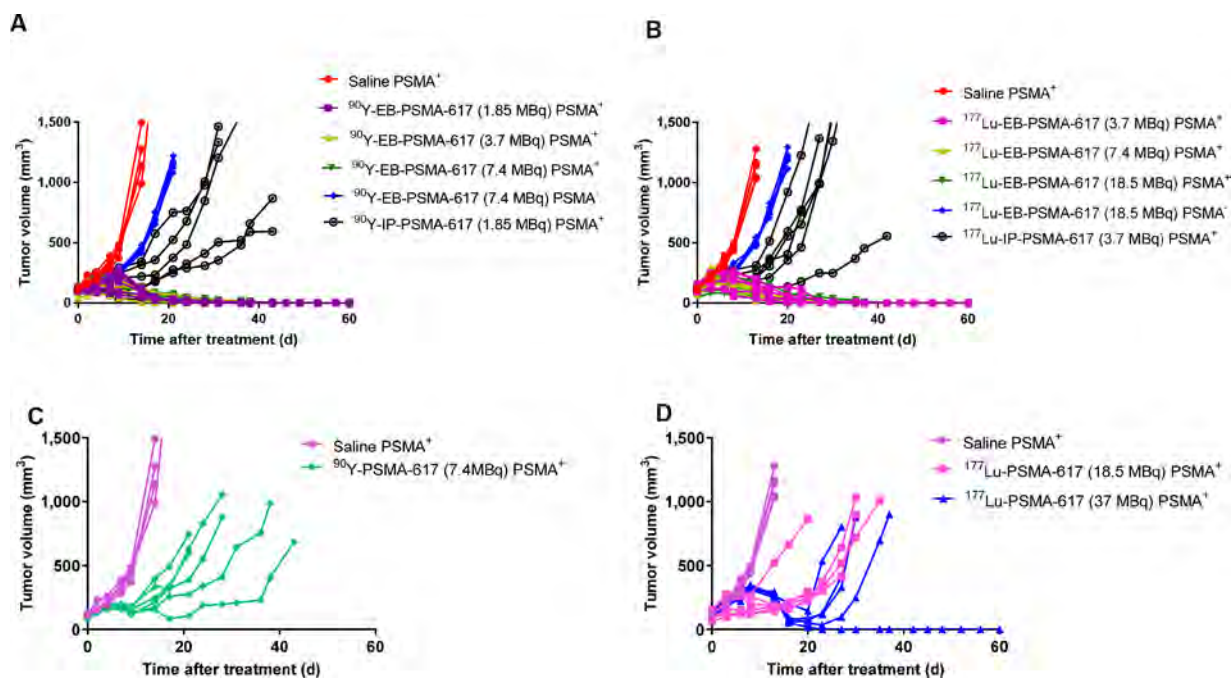

Figure 6. (A) Efficacy of radionuclide tumor therapy of mice bearing PSMA[+] or PSMA[−] tumors injected with a single dose of ^{90}Y-EB-PSMA-617/^{90}Y-IP-PSMA-617 (A) or ^{177}Lu-EB-PSMA-617/^{177}Lu-IP-PSMA-617 (B). (C, D) Injection of a single dose 7.4 MBq ^{90}Y-PSMA-617 (C) and 18.5 MBq or 37 MBq ^{177}Lu-PSMA-617 (D) to mice bearing PSMA[+] tumors. $P < 0.001$ for EB-PMSA-617 at all doses compared to saline, ^{90}Y-PSMA-617, and 18.5 MBq ^{177}Lu-PSMA-617.

efficacy in terms of tumor remission is not optimal.[1,25] One possibility for this limited efficacy is suboptimal pharmacoki-

netics, specifically rapid clearance from the blood. Small molecules work well for imaging PSMA due to the high signal-

Table 1. Complete Blood Counts from Mice Injected with 7.4 MBq ^{90}Y-EB-PSMA-617, 18.5 MBq ^{177}Lu-EB-PSMA-617 and Saline (Control) at the End Criteria or End of the Study[a]

	units	^{177}Lu-EB-PSMA-617 18.5 MBq		^{90}Y-EB-PSMA-617 7.4 MBq		control (saline)	
		average	STD	average	STD	average	STD
WBC	10^9/L	3.6	0.4	3.7	0.5	3.4	0.6
RBC	10^{12}/L	8.9	0.3	8.8	0.4	9.2	0.6
hemoglobin	g/L	123.9	8.7	121.2	9.3	128.4	12.3
platelets	10^9/L	887.2	172.1	896.3	143.6	918.2	150.2
MCV	fL	50.3	3.3	51.2	3.7	52.8	4.0
LYM #	10^9/L	1.7	0.2	1.6	0.3	1.6	0.2
MID #	10^9/L	1.2	0.3	1.3	0.3	1.3	0.2
GRAN #	10^9/L	4.6	0.5	5.2	0.6	5.4	0.7
LYM percentage	%	44.6	8.3	48.2	6.8	51.2	7.6
MID percentage	%	6.5	1.1	5.9	0.7	6.4	0.5
GRAN percentage	%	52.9	7.8	50.8	8.2	51.2	11.6

[a]Radioactive EB-PSMA does not induce hematotoxicity.

to-noise conferred by the rapid clearance but would limit the amount of radioligand delivered to the tumor.

We have previously used EB conjugation to substantially improve peptide receptor radionuclide therapy (PRRT) of neuroendocrine tumors expressing somatostatin receptor subtype-2 (SSTR2).[26] Following these encouraging results, herein we applied the same concept toward PSMA-617. PSMA-617 was to either EB or 4-(p-iodophenyl) (IP) moieties, which was shown to reversibly bind to albumin (Figure 1).[28]

EB-PSMA-617 (Figure 1) retained high affinity for PSMA compared to its parent molecule PSMA-617 (Figure 2B) and gained moderate affinity for albumin. The reversible binding to serum albumin significantly improved the pharmacokinetics of the radionuclide therapeutic agent and extended its blood half-life from merely minutes to several hours. Consequently, EB-PSMA-617 exhibited significantly higher uptake in PSMA$^+$ cells and xenograft tumors than PSMA-617 (Figures 3A and 5A).

An important requirement for a therapeutic radioligand is that the ligand be internalized by the cells so that the radioisotope can induce maximum damage from within the cells.[40] EB modification of PSMA-617 improved retention of the radionuclide within the cells after binding to the receptor and enhanced internalization (Figure 3). Although it is yet to be shown, we postulated that a fraction of PSMA-617 is recycled with the receptor and then washed off the receptor.[41] Surprisingly, the addition of EB seems to prevent or lower such recycling of the tracer, and a higher amount of the radioactivity is retained within the cells post receptor internalization. Therefore, by enhancing the uptake, internalization, and retention of radioactivity within the cells, we improved the therapeutic effect of PSMA-617 (Figure 6). By comparison, another albumin-binding version of PSMA-617, IP-PSMA-617, showed much less uptake and internalization than EB-PSMA-617 (Figures 3A,B).

Our in vivo PET imaging results corroborate the in vitro findings, which showed decreased tumor uptake over time for ^{86}Y-IP-PSMA-617 and ^{86}Y-PSMA-617 but increased tumor uptake for ^{86}Y-EB-PSMA-617 (Figures 4A,B and 5A). Comparable results for IP-PSMA were also reported by others.[29−33] ^{86}Y-EB-PSMA-617 and ^{86}Y-IP-PSMA-617 showed similar high blood retention at 1 h p.i., which was about 70-fold higher than that of ^{86}Y-PSMA-617. However, ^{86}Y-EB-PSMA-617 cleared much more slowly than ^{86}Y-IP-PSMA-617

over time, making it more available to bind PSMA in both target and nontarget organs, such as the tumor and kidneys.

We observed the kidney uptake of ^{86}Y-EB-PSMA-617 to be PSMA mostly specific based on our blocking studies, and there was no effective renal clearance over time. We examined possible increased damage caused by a high dose of ^{90}Y/^{177}Lu-EB-PSMA-617 to the kidneys and bone marrow compared to PSMA-617 due to the higher absorbed dose, but no pathologic abnormalities were observed (Figures S18 and S19). No changes in the blood chemistry were observed for either kidney or liver function, suggesting no damage to these organs. Moreover, first-in-human studies showed a lower tumor-to-kidney ratio than in mice, with an effective dose (mSv/MBq) of 5−6-fold higher for ^{177}Lu-EB-PSMA-617 than ^{177}Lu-PSMA-617. No significant toxicity to the kidneys nor the red bone marrow was observed and no changes in the blood chemistry for either kidneys or liver function, suggesting no damage to these organs.[42]

The high concentration of therapeutic ^{90}Y-EB-PSMA-617 or ^{177}Lu-EB-PSMA-617 in the tumors eradicated the tumor completely using a single dose administered per mouse (1.85 MBq ^{90}Y-EB-PSMA-617 and 3.7 MBq ^{177}Lu-EB-PSMA-617). As a comparison, a similar experiment done by us using an IP-derivative and a single dose of 3.7 MBq did not eradicate PSMA$^+$ tumors (Figure 6). Studies reported by Umbricht et al. on albumin-binding the ^{177}Lu-(tolyl)butyric acid conjugate to PSMA-617, with a higher dose of 5 MBq/mouse, led to complete tumor regression in four out of six mice bearing PSMA$^+$ xenografts.[30]

Clinically, PSMA expression by tumors is more heterogeneous. Additionally, there might be a threshold radioactivity concentration required to induce tumor regression. By delivering a significant amount of radiotherapeutic ^{90}Y/^{177}Lu-EB-PSMA, which is largely internalized, more PSMA$^+$ tumor cells and neighboring tumor cells are killed. Moreover, improving PSMA-617 pharmacokinetics by conjugation to EB may result in a lower dose of radioactivity injected and fewer injection cycles per patient, which in general will compensate for EB-PSMA-617's higher kidney uptake compared to multiple injection of PSMA-617 with higher doses.

F

CONCLUSIONS

We have prepared an analog of PSMA-617 containing truncated Evans blue albumin binding domain and a DOTA chelate to allow preparation of ^{86}Y, ^{90}Y, and ^{177}Lu for imaging and radiotherapy of PSMA in prostate cancer. The half-life in the blood was increased, resulting in enhanced tumor uptake and therapeutic efficacy when compared to radiolabeled PSMA-617. ^{90}Y- or ^{177}Lu-EB-PSMA induced complete remission in PMSA$^+$ xenograft mice with doses of 1.85 MBq/animal and 3.7 MBq/animal, respectively. No kidney, liver, or bone marrow toxicity was observed using pathology and blood chemistry analyses. We believe that these results justify studies in humans and expect ^{90}Y-/^{177}Lu-EB-PSMA-617 to demonstrate enhanced efficacy compared to ^{90}Y-/^{177}Lu-PSMA-617 while requiring lower doses and few cycles.

MATERIALS AND METHODS

General. Details of the organic syntheses, purification methods, and characterization of PSMA-617, EB-PSMA-617, and IP-PSMA-617 derivatives are described in the Supporting Information. The immunofluorescence staining protocol of excised tumors is outlined in the Supporting Information.

Radiolabeling. ^{86}Y was obtained from the NIH Cyclotron Facility. ^{90}Y was purchased from PerkinElmer. ^{177}Lu was purchased from the University of Missouri Research Reactor. A stock solution of the isotopes (370−740 MBq) was mixed with 0.5−1 mL of 0.4 M ammonium acetate (pH 5.6). PSMA-617, EB-PSMA-617, or IP-PSMA-617 (25−50 nmol in 10 μL volume of dimethyl sulfoxide (DMSO)) was added to 185−370 MBq of the isotopes mentioned above. The reaction mixture was incubated on a thermomixer with 800 rpm agitation at 80 °C for 30 min. Complete complexation of the metal into the chelator was shown using radio-thin-layer chromatography (AR-2000 Bioscan scanner), with iTLC plates (Fisher) and 0.1 M citric acid (pH 5) as a mobile phase. The R_f of free radiometal ∼ 0.7−0.9; the R_f of the labeled ligand ∼ 0.1−0.3.

Cell Culture. PC3 (human prostate cancer, PSMA$^-$) cells were obtained from American Type Culture Collection. PC3-PIP (PSMA$^+$) cells were kindly provided by Dr. Martin G. Pomper (Johns Hopkins University). The cells were cultured in RPMI-1640 with 10% fetal bovine serum in a humidified incubator containing 5% CO_2 at 37 °C.

Flow Cytometry Analysis. A total of 1×10^6 cells/mL of PSMA$^+$ and PSMA$^-$ cells in 1% bovine serum albumin (BSA)/phosphate buffered saline (PBS) were used for this study and kept at 4 °C at all times. The cells were seeded in 75 cm^2 flasks and incubated with 10 μL of either anti-PSMA and/or isotype control (R&D Systems) for 0.5 h. Then, the cells were washed three times with PBS and the fluorescence was read on Accuri C6 plus cytometer (BD Biosciences). Analysis of the results was done using FlowJo (Tristar).

Cell Binding Assays. A cell binding assay was done in a membrane 96-well plate (Millipore) at room temperature (RT) using PBS as a solvent and increasing concentrations of EB-PSMA-617, IP-PSMA-617, and PSMA-617 (0−500 nM). A total of 3.7 kBq of ^{86}Y-PSMA-617 was added to each well followed by the addition of 10^5 PSMA$^+$ cells. After 1−2 h of incubation with moderate shaking at RT, the cells were washed three times with PBS, and the membrane was dried on a heater for 15 min. The samples were counted on a gamma counter (PerkinElmer), and the data were analyzed in GraphPad Prism

using nonlinear regression. This study was repeated twice in triplicate.

Uptake, Internalization, and Efflux Assays. A total of 10^5 cells were plated in a 24-well plate 24 h before the experiment in supplemented media. Before adding the radioligand, the medium was removed, and then ^{86}Y-EB-PSMA-617, ^{86}Y-IP-PSMA-617, or ^{86}Y-PSMA-617 (37 kBq in 0.5 mL of medium containing 1% human serum albumin (HSA)) was added. The plates were incubated at 37 °C for 1, 4, and 24 h. A total of 10 μg of unlabeled ligand was added to the blocking designated wells. For the uptake experiment, at each time point, the medium was removed, and the wells were washed with 1 mL of PBS, followed by adding 0.2 mL of 1 M NaOH to facilitate cell lysis. An internalization assay was performed by adding 0.5 mL of acid medium (50 mM glycine, 100 mM NaCl, pH 2.8) for 1 min. After the removal of the radioactivity, the wells were rinsed again with PBS, and 0.2 mL of 1 M NaOH was added. For efflux studies, the plates containing the radioligand in the 1% HSA medium were incubated for 4 h at 37 °C. Then, the solvent was removed, and the wells were rinsed with 1 mL of PBS, followed by the addition of 0.5 mL of medium without albumin. The plates were incubated at 37 °C for 4 and 24 h, and cell lysates were extracted as mentioned above. Cell lysates for all the studies were collected and counted in a gamma counter. These assays were repeated twice in triplicate, and analysis was done using Excel and GraphPad Prism.

Tumor Xenograft Model. All animal studies were performed in compliance with the NIH Clinical Center Animal Care and Use Committee. Mouse studies were conducted in 7−8 week old athymic nude male mice (Envigo). Tumors were implanted subcutaneously on the right shoulder with 5×10^6 PC3-PIP (PSMA$^+$) or PC-3 (PSMA$^-$) cells using Matrigel 1:1, in a total volume of 0.1 mL. The tumors were allowed to grow to reach a volume of 300−350 mm^3 for PET and 100−160 mm^3 for radiotherapy studies.

PET and Biodistribution Studies. Mice were injected intravenously with 3.7−5.1 MBq (1 nmol) of ^{86}Y-EB-PSMA-617 ($n = 5$), ^{86}Y-IP-PSMA-617 ($n = 5$), or ^{86}Y-PSMA-617 ($n = 5$) in saline, and PET scans were obtained at 1, 4, 24, and 48 h post injection (p.i.) using an Inveon small animal PET scanner (Siemens Preclinical Solutions) and/or Nanoscan-PET/CT (Mediso). Acquisition time for each scan was 10−20 min. The images were reconstructed using ASIPRO (Siemens Preclinical Solutions) and/or VivoQuant (Invicro). Blocking studies for kidney uptake were done in Balb/c male mice (10-weeks old, $n = 4$/group) by injection of 925 kBq ^{86}Y-EB-PSMA-617 with or without unlabeled EB-PSMA-617 (200-fold excess).

Biodistribution was carried out after the last PET scan time point. Mice were sacrificed, and the tumor, heart, lung, liver, spleen, stomach, intestine, pancreas, kidneys, muscle, bone, and blood were harvested and wet weighed. The amount of radioactivity was determined by a gamma counter. Results are expressed as percentages of the injected dose per gram of tissue (% ID/g).

Radiotherapy Studies of EB-PSMA-617 and PSMA-617 Using Y-90 and Lu-177. Tumor volume (mm^3) was calculated as (length (mm) × width (mm)^2)/2. Tumor volume, body weight, and survival rate were monitored every 2−3 days until the end of the study (60 days). Mice were randomized into 12 groups: saline ($n = 6$), 1.85 MBq ^{90}Y-EB-PSMA-617 ($n = 8$), 3.7 MBq ^{90}Y-EB-PSMA-617 ($n = 10$), 7.4 MBq ^{90}Y-EB-PSMA-617 ($n = 10$), 3.7 MBq ^{177}Lu-EB-PSMA-

617 (n = 8), 7.4 MBq ^{177}Lu-EB-PSMA-617 (n = 10), 18.5 MBq ^{177}Lu-EB-PSMA-617 (n = 10), 7.4 MBq ^{90}Y-PSMA-617 (n = 6), 18.5 MBq ^{177}Lu- PSMA-617 (n = 6), 37 MBq ^{177}Lu-PSMA-617 (n = 6), 1.85 MBq ^{90}Y-IP-PSMA-617 (n = 6), or 3.7 MBq ^{177}Lu-IP-PSMA-617 (n = 6). The mice were euthanized once tumor volume reached over 1800 mm^3 or when tumors began to ulcerate.

Blood Count Test. Blood samples were collected through the mouse tail vein and kept in heparin-treated tubes. Blood count tests were carried out with a hematology analyzer (PLA1000, Pro-Lab Diagnostics) following the vendor protocol.

Statistical Analysis. Results were shown with mean ± SD. The differences within groups and between groups were determined with two-tailed paired and unpaired Student's t tests, respectively.

■ ASSOCIATED CONTENT

Ⓢ Supporting Information

The Supporting Information is available free of charge on the ACS Publications website at DOI: 10.1021/acs.bioconjchem.8b00556.

Materials and Methods and Figures S1−S19 (PDF)

■ AUTHOR INFORMATION

Corresponding Authors
*E-mail: orit.jacobsonweiss@nih.gov. Phone: 301-435-2229.
*E-mail: Shawn.chen@nih.gov. Phone: 301-451-4246.

ORCID Ⓞ
Xiaoyuan Chen: 0000-0002-9622-0870

Notes
The authors declare no competing financial interest.

■ ACKNOWLEDGMENTS

■ REFERENCES

(1) Emmett, L., Willowson, K., Violet, J., Shin, J., Blanksby, A., and Lee, J. (2017) Lutetium (177) PSMA radionuclide therapy for men with prostate cancer: a review of the current literature and discussion of practical aspects of therapy. *J. Med. Radiat Sci.* 64, 52−60.

(2) Hillier, S. M., Maresca, K. P., Femia, F. J., Marquis, J. C., Foss, C. A., Nguyen, N., Zimmerman, C. N., Barrett, J. A., Eckelman, W. C., Pomper, M. G., Joyal, J. L., and Babich, J. W. (2009) Preclinical evaluation of novel glutamate-urea-lysine analogues that target prostate-specific membrane antigen as molecular imaging pharmaceuticals for prostate cancer. *Cancer Res.* 69, 6932−6940.

(3) Eiber, M., Fendler, W. P., Rowe, S. P., Calais, J., Hofman, M. S., Maurer, T., Schwarzenboeck, S. M., Kratowchil, C., Herrmann, K., and Giesel, F. L. (2017) Prostate-Specific Membrane Antigen Ligands for Imaging and Therapy. *J. Nucl. Med.* 58, 67S−76S.

(4) Schwarzenboeck, S. M., Rauscher, I., Bluemel, C., Fendler, W. P., Rowe, S. P., Pomper, M. G., Asfhar-Oromieh, A., Herrmann, K., and Eiber, M. (2017) PSMA Ligands for PET Imaging of Prostate Cancer. *J. Nucl. Med.* 58, 1545−1552.

(5) Lutje, S., Slavik, R., Fendler, W., Herrmann, K., and Eiber, M. (2017) PSMA ligands in prostate cancer - Probe optimization and theranostic applications. *Methods* 130, 42−50.

(6) Bouchelouche, K., Choyke, P. L., and Capala, J. (2010) Prostate specific membrane antigen-a target for imaging and therapy with radionuclides. *Discovery Med.* 9, 55−61.

(7) Lutje, S., Heskamp, S., Cornelissen, A. S., Poeppel, T. D., van den Broek, S. A. M. W., Rosenbaum-Krumme, S., Bockisch, A., Gotthardt, M., Rijpkema, M., Boerman, O. C., et al. (2015) PSMA Ligands for Radionuclide Imaging and Therapy of Prostate Cancer: Clinical Status. *Theranostics* 5, 1388−1401.

(8) Baccala, A., Sercia, L., Li, J., Heston, W., and Zhou, M. (2007) Expression of prostate-specific membrane antigen in tumor-associated neovasculature of renal neoplasms. *Urology* 70, 385−390.

(9) Cho, S. Y., Gage, K. L., Mease, R. C., Senthamizhchelvan, S., Holt, D. P., Jeffrey-Kwanisai, A., Endres, C. J., Dannals, R. F., Sgouros, G., Lodge, M., et al. (2012) Biodistribution, tumor detection, and radiation dosimetry of 18F-DCFBC, a low-molecular-weight inhibitor of prostate-specific membrane antigen, in patients with metastatic prostate cancer. *J. Nucl. Med.* 53, 1883−1891.

(10) Chatalic, K. L., Heskamp, S., Konijnenberg, M., Molkenboer-Kuenen, J. D., Franssen, G. M., Clahsen-van Groningen, M. C., Schottelius, M., Wester, H. J., van Weerden, W. M., Boerman, O. C., and de Jong (2016) Towards Personalized Treatment of Prostate Cancer: PSMA I&T, a Promising Prostate-Specific Membrane Antigen-Targeted Theranostic Agent. *Theranostics* 6, 849−861.

(11) Maurer, T., Weirich, G., Schottelius, M., Weineisen, M., Frisch, B., Okur, A., Kubler, H., Thalgott, M., Navab, N., Schwaiger, M., et al. (2015) Prostate-specific membrane antigen-radioguided surgery for metastatic lymph nodes in prostate cancer. *Eur. Urol.* 68, 530−534.

(12) Weineisen, M., Schottelius, M., Simecek, J., Baum, R. P., Yildiz, A., Beykan, S., Kulkarni, H. R., Lassmann, M., Klette, I., Eiber, M., et al. (2015) 68Ga- and 177Lu-Labeled PSMA I&T: Optimization of a PSMA-Targeted Theranostic Concept and First Proof-of-Concept Human Studies. *J. Nucl. Med.* 56, 1169−1176.

(13) Vallabhajosula, S., Goldsmith, S. J., Kostakoglu, L., Milowsky, M. I., Nanus, D. M., and Bander, N. H. (2005) Radioimmunotherapy of prostate cancer using 90Y- and 177Lu-labeled J591 monoclonal antibodies: effect of multiple treatments on myelotoxicity. *Clin. Cancer Res.* 11, 7195s−7200s.

(14) Vallabhajosula, S., Goldsmith, S. J., Hamacher, K. A., Kostakoglu, L., Konishi, S., Milowski, M. I., Nanus, D. M., and Bander, N. H. (2005) Prediction of myelotoxicity based on bone marrow radiation-absorbed dose: radioimmunotherapy studies using 90Y- and 177Lu-labeled J591 antibodies specific for prostate-specific membrane antigen. *J. Nucl. Med.* 46, 850−858.

(15) Bander, N. H., Milowsky, M. I., Nanus, D. M., Kostakoglu, L., Vallabhajosula, S., and Goldsmith, S. J. (2005) Phase I trial of 177lutetium-labeled J591, a monoclonal antibody to prostate-specific membrane antigen, in patients with androgen-independent prostate cancer. *J. Clin. Oncol.* 23, 4591−4601.

(16) Wilkinson, S., and Chodak, G. (2004) An evaluation of intermediate-dose ketoconazole in hormone refractory prostate cancer. *Eur. Urol.* 45, 581−584 discussion 585..

(17) Bander, N. H. (2006) Technology insight: monoclonal antibody imaging of prostate cancer. *Nat. Clin. Pract. Urol.* 3, 216−225.

(18) Kozikowski, A. P., Nan, F., Conti, P., Zhang, J., Ramadan, E., Bzdega, T., Wroblewska, B., Neale, J. H., Pshenichkin, S., and Wroblewski, J. T. (2001) Design of remarkably simple, yet potent urea-based inhibitors of glutamate carboxypeptidase II (NAALA-Dase). *J. Med. Chem.* 44, 298−301.

(19) Maresca, K. P., Hillier, S. M., Femia, F. J., Keith, D., Barone, C., Joyal, J. L., Zimmerman, C. N., Kozikowski, A. P., Barrett, J. A., Eckelman, W. C., et al. (2009) A series of halogenated heterodimeric inhibitors of prostate specific membrane antigen (PSMA) as radiolabeled probes for targeting prostate cancer. *J. Med. Chem.* 52, 347−357.

(20) Rajasekaran, S. A., Anilkumar, G., Oshima, E., Bowie, J. U., Liu, H., Heston, W., Bander, N. H., and Rajasekaran, A. K. (2003) A novel cytoplasmic tail MXXXL motif mediates the internalization of prostate-specific membrane antigen. *Mol. Biol. Cell* 14, 4835−4845.

(21) Ghosh, A., and Heston, W. D. (2004) Tumor target prostate specific membrane antigen (PSMA) and its regulation in prostate cancer. *J. Cell. Biochem. 91*, 528−539.

(22) Rahbar, K., Boegemann, M., Yordanova, A., Eveslage, M., Schafers, M., Essler, M., and Ahmadzadehfar, H. (2018) PSMA targeted radioligandtherapy in metastatic castration resistant prostate cancer after chemotherapy, abiraterone and/or enzalutamide. A retrospective analysis of overall survival. *Eur. J. Nucl. Med. Mol. Imaging 45*, 12−19.

(23) Rahbar, K., Bogeman, M., Yordanova, A., Eveslage, M., Schafers, M., Essler, M., and Ahmadzadehfar, H. (2018) Delayed response after repeated (177)Lu-PSMA-617 radioligand therapy in patients with metastatic castration resistant prostate cancer. *Eur. J. Nucl. Med. Mol. Imaging 45*, 243−246.

(24) Hofman, M. S., Violet, J., Hicks, R. J., Ferdinandus, J., Thang, S. P., Akhurst, T., Iravani, A., Kong, G., Ravi Kumar, A., Murphy, D. G., et al. (2018) [(177)Lu]-PSMA-617 radionuclide treatment in patients with metastatic castration-resistant prostate cancer (LuPSMA trial): a single-centre, single-arm, phase 2 study. *Lancet Oncol. 19*, 825−833.

(25) Baum, R. P., Kulkarni, H. R., Schuchardt, C., Singh, A., Wirtz, M., Wiessalla, S., Schottelius, M., Mueller, D., Klette, I., and Wester, H. J. (2016) 177Lu-Labeled Prostate-Specific Membrane Antigen Radioligand Therapy of Metastatic Castration-Resistant Prostate Cancer: Safety and Efficacy. *J. Nucl. Med. 57*, 1006−1013.

(26) Kulkarni, H. R., Singh, A., Schuchardt, C., Niepsch, K., Sayeg, M., Leshch, Y., Wester, H. J., and Baum, R. P. (2016) PSMA-Based Radioligand Therapy for Metastatic Castration-Resistant Prostate Cancer: The Bad Berka Experience Since 2013. *J. Nucl. Med. 57*, 97S−104S.

(27) Muller, C., Struthers, H., Winiger, C., Zhernosekov, K., and Schibli, R. (2013) DOTA conjugate with an albumin-binding entity enables the first folic acid-targeted 177Lu-radionuclide tumor therapy in mice. *J. Nucl. Med. 54*, 124−131.

(28) Siwowska, K., Haller, S., Bortoli, F., Benesova, M., Groehn, V., Bernhardt, P., Schibli, R., and Muller, C. (2017) Preclinical Comparison of Albumin-Binding Radiofolates: Impact of Linker Entities on the in Vitro and in Vivo Properties. *Mol. Pharmaceutics 14*, 523−532.

(29) Benesova, M., Umbricht, C. A., Schibli, R., and Muller, C. (2018) Albumin-Binding PSMA Ligands: Optimization of the Tissue Distribution Profile. *Mol. Pharmaceutics 15*, 934−946.

(30) Umbricht, C. A., Benesova, M., Schibli, R., and Muller, C. (2018) Preclinical Development of Novel PSMA-Targeting Radioligands: Modulation of Albumin-Binding Properties To Improve Prostate Cancer Therapy. *Mol. Pharmaceutics 15*, 2297−2306.

(31) Choy, C. J., Ling, X., Geruntho, J. J., Beyer, S. K., Latoche, J. D., Langton-Webster, B., Anderson, C. J., and Berkman, C. E. (2017) 177)Lu-Labeled Phosphoramidate-Based PSMA Inhibitors: The Effect of an Albumin Binder on Biodistribution and Therapeutic Efficacy in Prostate Tumor-Bearing Mice. *Theranostics 7*, 1928−1939.

(32) Kelly, J., Amor-Coarasa, A., Ponnala, S., Nikolopoulou, A., Williams, C., Jr., Schlyer, D., Zhao, Y., Kim, D., and Babich, J. W. (2018) Trifunctional PSMA-Targeting Constructs for Prostate Cancer with Unprecedented Localization to LNCaP Tumors. *Eur. J. Nucl. Med. Mol. Imaging*, DOI: 10.1007/s00259-018-4004-5.

(33) Kelly, J. M., Amor-Coarasa, A., Nikolopoulou, A., Wustemann, T., Barelli, P., Kim, D., Williams, C., Jr., Zheng, X., Bi, C., Hu, B., et al. (2017) Dual-Target Binding Ligands with Modulated Pharmacokinetics for Endoradiotherapy of Prostate Cancer. *J. Nucl. Med. 58*, 1442−1449.

(34) Chen, H., Jacobson, O., Niu, G., Weiss, I. D., Kiesewetter, D. O., Liu, Y., Ma, Y., Wu, H., and Chen, X. (2017) Novel "Add-On" Molecule Based on Evans Blue Confers Superior Pharmacokinetics and Transforms Drugs to Theranostic Agents. *J. Nucl. Med. 58*, 590−597.

(35) Tian, R., Jacobson, O., Niu, G., Kiesewetter, D. O., Wang, Z., Zhu, G., Ma, Y., Liu, G., and Chen, X. (2018) Evans Blue Attachment Enhances Somatostatin Receptor Subtype-2 Imaging and Radiotherapy. *Theranostics 8*, 735−745.

(36) Benesova, M., Schafer, M., Bauder-Wust, U., Afshar-Oromieh, A., Kratochwil, C., Mier, W., Haberkorn, U., Kopka, K., and Eder, M. (2015) Preclinical Evaluation of a Tailor-Made DOTA-Conjugated PSMA Inhibitor with Optimized Linker Moiety for Imaging and Endoradiotherapy of Prostate Cancer. *J. Nucl. Med. 56*, 914−920.

(37) Sugiura, G., Kuhn, H., Sauter, M., Haberkorn, U., and Mier, W. (2014) Radiolabeling strategies for tumor-targeting proteinaceous drugs. *Molecules 19*, 2135−2165.

(38) Tornesello, A. L., Buonaguro, L., Tornesello, M. L., and Buonaguro, F. M. (2017) New Insights in the Design of Bioactive Peptides and Chelating Agents for Imaging and Therapy in Oncology. *Molecules 22*, 1282.

(39) Kinoshita, Y., Kuratsukuri, K., Landas, S., Imaida, K., Rovito, P. M., Jr., Wang, C. Y., and Haas, G. P. (2006) Expression of Prostate-Specific Membrane Antigen in Normal and Malignant Human Tissues. *World J. Surg. 30*, 628−636.

(40) Kersemans, V. (2010) Targeted Molecular Radiotherapy. *Curr. Drug Discovery Technol. 7*, 232.

(41) Ghosh, A., Wang, X., Klein, E., and Heston, W. D. (2005) Novel Role of Prostate-Specific Membrane Antigen in Suppressing Prostate Cancer Invasiveness. *Cancer Res. 65*, 727−731.

(42) Zang, J., Fan, X., Wang, H., Liu, Q., Wang, J., Li, H., Li, F., Jacobson, O., Niu, G., Zhu, Z., and Chen, X. (2018) First-in-Human Study of 177Lu-EB-PSMA-617 in Patients with Metastatic Castration-Resistant Prostate Cancer, *Eur. J. Nucl. Med. Mol. Imaging*, DOI: 10.1007/s00259-018-4096-y.